Progress In Electromagnetics Research, Vol. 158, 89–98, 2017

Millimeter Wave Cavity Backed Microstrip Antenna Array for 79 GHz Radar Applications

Mohammad Mosalanejad[1, 2, *], Steven Brebels[2], Charlotte Soens[2], Ilja Ocket[1, 2], and Guy A. E. Vandenbosch[1]

Abstract—In this paper, a 79 GHz microstrip antenna subarray, optimized for operation in a Phase Modulated Continuous Wave (PMCW) MIMO radar demonstrator is presented. The antenna combines all necessary features for this very specific type of applications. First of all, the spillover between transmit and receive channels in such a system is reduced by the combined effect of a microvia cage and the arraying of two elements. Second, it shows a wide band of 13.5%. Third, a wide beam in the E-plane (136 degrees), necessary for scanning, and a much smaller beamwidth in H-plane (36 degrees), advantageous to reduce mutual coupling, are realized. Finally, it has been fabricated with the advanced so-called "Any-Layer" technology. This technology is as accurate as other advanced technologies in the millimeter wave bands, but at a much lower cost, and thus very suited for mass production. The gain and radiation efficiency were simulated to be 7.44 dBi and 83%, respectively.

1. INTRODUCTION

Millimeter wave (MMW) applications have become increasingly important in recent years, both in communications and in sensing [1, 2]. The latter is currently dominated by automotive radar, but it is expected that millimeter wave sensing applications are to follow the growth of millimeter wave communications. As CMOS is emerging as a viable technology for 79 GHz radar systems and beyond, lower system cost will be the result [3].

Designing antennas in the millimeter wave band is challenging, not only because of the design methodology needed to achieve high performance, but also because of the fabrication technology, complexity and cost. Moreover, these antennas must be easy to integrate in packages. For millimeter wave commercial products like automotive radars, MMW antennas must be low cost, have high gain and high integration ability for mass production.

In PMCW (Phase Modulated Continuous Wave) radars, where transmission and reception of all signal frequencies occur continuously, low mutual coupling between transmitter and receiver elements is extremely important, to avoid overwhelming the receiver system [4]. Different methods have been reported in literature to reduce mutual coupling. These methods include changing the shape of the patch elements [5, 6], using defected ground structures (DGS) [7, 8], and utilizing electromagnetic band gap structures (EBG) [9], and other metamaterials [10, 11]. Although these methods are quite effective, they typically have low bandwidth and are often difficult to manufacture reliably. Surrounding the radiating elements by a metallic cavity [12, 13] is another way to suppress mutual coupling. This technique is more amenable to fabrication in PCB technology, albeit in the most advanced types. Also, it does not suffer from low bandwidth and since surface waves are not excited in the substrate, the radiation efficiency is also enhanced. And finally, since the fringing fields between the patch and the cavity occur

Received 4 January 2017, Accepted 23 March 2017, Scheduled 9 April 2017

* Corresponding author: Mohammad Mosalanejad (mohammad.mosalanejad@esat.kuleuven.be).

[1] KU Leuven, Div. ESAT-TELEMIC, Kasteelpark Arenberg 10, B-3001, Leuven, Belgium. [2] IMEC, SSET/CSI, Kapeldreef 75, B-3001 Leuven, Belgium.

in a small region, such patch antennas have broader beams compared to their counterparts without a shielding cavity. For short range radars, this characteristic is especially beneficial.

Various technologies have been reported as being suitable for MMW antennas, each with their own advantages and disadvantages. LTCC (low-temperature co-fired ceramic) [14] offers low loss and high design freedom through the high possible number of layers, but at high cost and high relative permittivity. In addition, this technology requires temperatures above 850 degrees Celsius. At this temperature active devices are completely destroyed. So in contrast to passive devices, active devices have to be integrated into the package after the firing process. LCP (Liquid Crystal Polymer) [15] offers very low loss at low permittivity, but is difficult to laminate. Moreover, it has to be used in mixed stack-ups with other substrates like FR4 or Rogers RO4000. The main reason is that in LCP, grass cloth cannot be used to keep x-y coordinates exactly in place during the fabrication process. Teflon based PCB technology is a another advanced technology in millimeter wave bands [18], but it is again very costly and hard to fabricate. Another disadvantage with both LCP and Teflon based PCB is that they work with layers with considerably different CTE (Coefficient Temperature Expansion). Therefore, when the temperature rises the PCB board tends to bend, and there is a serious possibility that microvias crack or that the metals depart from the board. Hence, with LCP or Teflon based technologies, usually it is not possible to reach more than 8–10 layers. Nowadays, advanced PCB technologies are emerging that offer high layer-count stack-ups and narrow pitch microvias as in LTCC and LCP, but using low permittivity materials and at a much lower cost. The cost can be decreased with a factor 3 in mass production. In this paper, such a stack-up is used.

In millimeter wave radars, there is a quite strict set of requirements. First, in order to avoid the effect of grating lobes, the distance between array elements must be less than half a wavelength, which results in quite small elements. Second, the mutual coupling between array elements must be as low as possible. Third, aiming at higher production volumes in a consumer market, the cost of fabrication has to be as low as possible. Designing and fabricating antennas that satisfy all these requirements is challenging. In literature, a number of examples have been published of cavity backed MMW microstrip antennas. In [14], a 60 GHz LTCC patch antenna backed by an air-filled cavity was reported. In addition to the expensive LTCC technology used, embedding air into the stack-up increases the fabrication complexity and cost even further. Moreover, no solution has been considered to suppress the surface waves in the multi-layer build-up. In [16], a 60 GHz open waveguide cavity backed LTCC antenna package is reported. Again, the fabrication technology is costly, and also the size of the array elements is bigger than half a wavelength. In [15] and [17], aperture coupled patch antennas have been used in LCP and MLO (Multi Layer Organic) technologies, respectively, with very costly air cavities embedded into the stack-up. In [18], a cavity backed horn-type antenna-in-package has been presented. This antenna has been fabricated in a Teflon based PCB technology and has a wide bandwidth of 24.8%. However, again the manufacturing cost is high and the antenna element is bigger than half a wavelength. A brief comparison between our work and other antennas published in open literature is made in Table 1.

Table 1. Comparison to multilayer antennas in literature.

Reference	14	16	17	18	This work
Frequency	60 GHz	60 GHz	60 GHz	60 GHz	79 GHz
Technology	LTCC	LTCC	MLO	Teflon based PCB	Any-Layer PCB
Cost	High	High	High	High	Low
Element size	$< \lambda/2$	$> \lambda/2$	$< \lambda/2$	$> \lambda/2$	$< \lambda/2$
Embedding Air cavity	Yes	No	Yes	No	No
Spillover suppression	No	Yes	No	Yes	Yes

In this paper, we present a cavity backed 79 GHz stacked patch antenna with very low mutual coupling and reduced antenna loss due to the avoidance of substrate waves. As far as we can see, this antenna satisfies all the necessary features for a millimeter wave MIMO radar (low mutual coupling, compact size less than half a wavelength, and cheap fabrication) in a superior way compared to all the topologies already published in literature. The antenna has been fabricated with a newly introduced

"Advanced Any-Layer PCB" technology. This technology is as accurate as other advanced technologies but at a much lower cost. Moreover, a wideband feed transition has been designed to feed the antenna through a multi-layer board, also acting as a matching circuit. In the next section, the "Any-Layer" technology and its benefits over other expensive technologies will be described. Then, the antenna topology will be described. Finally the measurement results will be discussed.

2. PCB TECHNOLOGY, LAYER BUILD-UP AND MATERIALS

The PCB technology that is exploited is referred to as "Any-Layer Technology" [23]. The Any-Layer Technology is an advancement of "Standard" existing HDI (High Density Interconnect) micro-via technology in printed circuit boards. With Any-Layer Technology, all electrical connections between the individual printed circuit board layers are formed by laser-drilled micro-vias, the micro-vias are copper filled and stacked. This gives the design community optimum design freedom as each layer or connection on a specific layer can be connected to every other layer within the PCB stack-up. In general, conventional through holes are eliminated by this process and replaced by micro-via holes. The features that go with this are quite a bit smaller than the features required for conventionally drilled, blind, or through holes. There is also an extensive space saving opportunity and the possibility to reduce size, layer-count and/or weight of a product. For a given product dimension, an increased routing density is possible. A cross section of a PCB board fabricated by this technology is depicted in Fig. 1. Also, a comparison between this multilayer PCB and LTCC is made in Table 2. In fact, this technology is almost as accurate as LTCC, but at an much lower cost. It is worth mentioning that, to the knowledge of authors, this is the first time that this advanced multi-layer PCB technology is used in the design and fabrication of a batch of millimeter wave antennas.

The layer build-up that is actually used for the antenna fabrication is shown in Fig. 2. This build-up shows a perfect symmetry along the substrate thickness direction. 8 metal layers are used. Layers 3 and

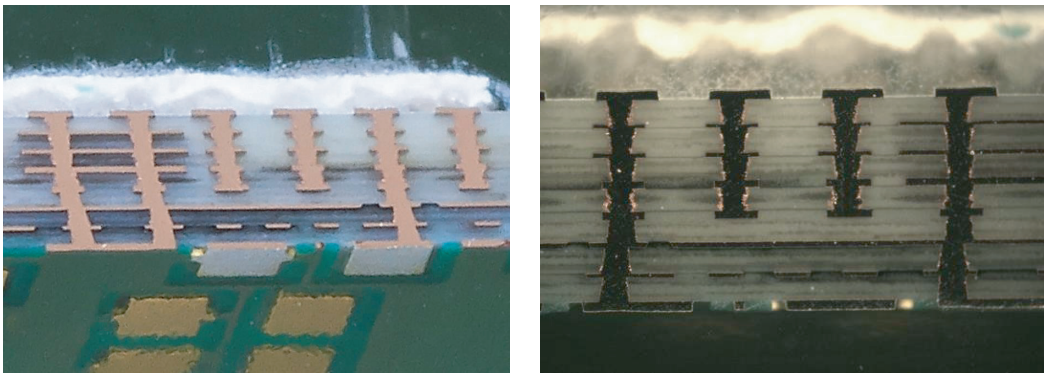

(a) (b)

Figure 1. 3D view of Any-layer PCB cross section. The stacked microvias can be clearly seen.

Table 2. A comparison between any-layer PCB, and LTCC.

Characteristics	Any-Layer PCB	LTCC
Minimum substrate thickness (μm)	50	50
Minimum track width (μm)	50	35
Minimum micro-via diameter (μm)	70	50
Minimum clearance between tracks (μm)	50	35
Cost	Less	More
Fabrication ease	Easier	Harder

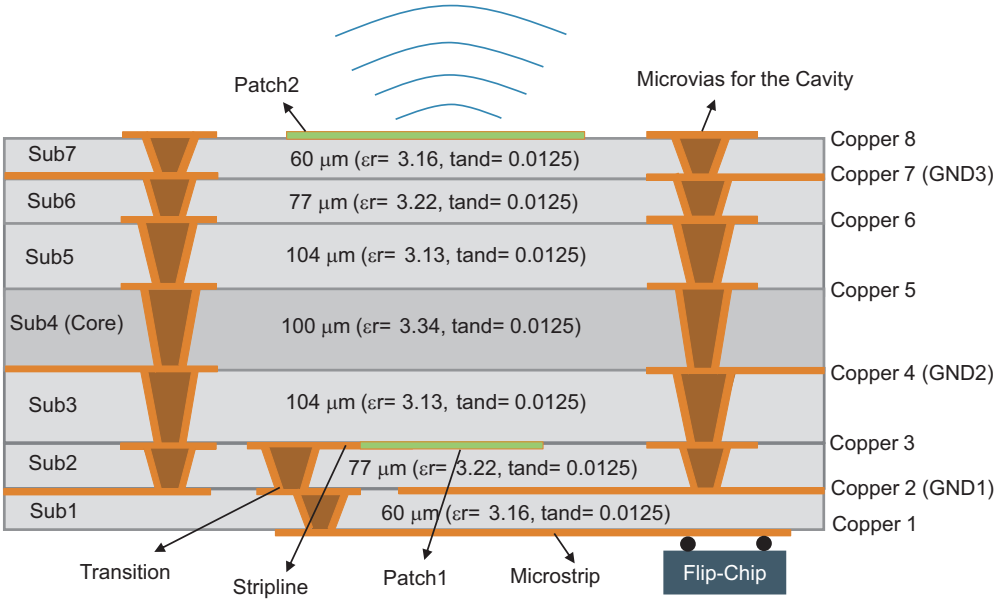

Figure 2. Layer build-up used to implement the antenna sub-array.

8 are used for the stacked patches, layers 2, 4 and 7 as ground planes, and the transition from microstrip to stripline is done between layers 1 and 3. In the final radar module, layers 1, 3, 5 and 6 are also used for routing the tracks for the different signals. The thickness of all metal layers is around 25 micrometers. Further, 7 different substrates are used. All of the laminate and prepreg materials for the substrates are of the Panasonic Megtron 6 type. Their characteristics are given in Fig. 2. The permittivity of all these dielectrics is higher than 3. Lower permittivity materials yield a higher bandwidth, but it is hard to find and use such materials for millimeter wave applications. On top, they are very costly. Small micro-vias are used in substrates 2–7 to make the cavities around the patches.

3. ANTENNA SUB-ARRAY

The designed antenna sub-array is composed of 2 elements in the H-plane which are fed through a corporate feed. The elements are put in each other's H-plane to make the beamwidth narrower in this plane.

The narrower pattern in this plane will lead to lower mutual coupling between the Tx and Rx elements in the radar module. For this antenna sub-array, a wide band feed transition from microstrip

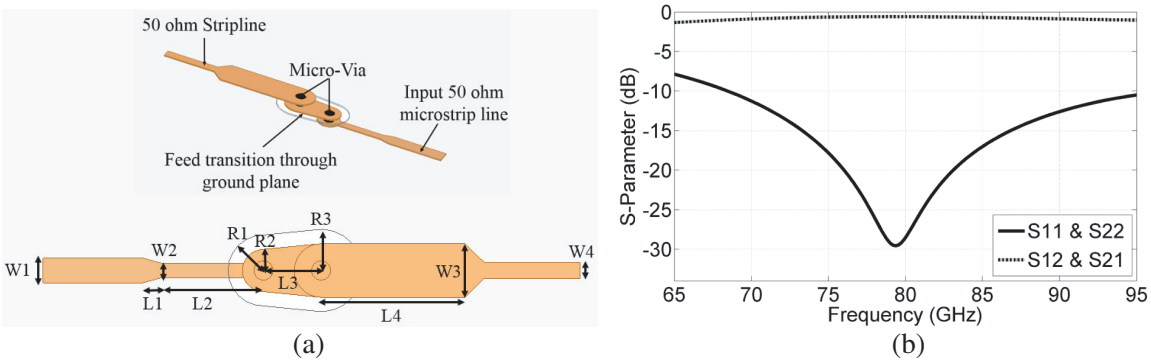

Figure 3. (a) Microstrip to stripline transition: $W1 = 0.13\,\text{mm}$, $W2 = 0.075\,\text{mm}$, $L2 = 0.53\,\text{mm}$, $W3 = 0.28\,\text{mm}$, $L3 = 0.75\,\text{mm}$, $W4 = 0.085\,\text{mm}$, $Lt1 = 0.1\,\text{mm}$, $Lt2 = 0.3\,\text{mm}$, $Lt3 = 0.1\,\text{mm}$, $R1 = 0.185\,\text{mm}$, $R2 = 0.11\,\text{mm}$, $R3 = 0.2\,\text{mm}$. (b) Scattering parameters.

to stripline is designed. This feed transition and it's S-parameters are shown in Fig. 3. In the frequency band 77–81 GHz the transition has around 0.6 dB loss and a reflection coefficient lower than −20 dB. In addition, this transition helps us to feed the antenna through GND1. The bottom patch radiation to the chip side of the package is reduced considerably by the GND1 layer. The transition also acts as a matching network for the antenna sub-array. The geometry of the sub-array and all dimensions are shown in Fig. 4. Note that the dimensions of the transition there are not exactly the same as the ones in Fig. 3. The slight differences are due to the further optimization performed on the sub-array in order to get a better S_{11} matching.

The geometry of the sub-array and all dimensions are shown in Fig. 4. As mentioned before, the feed transition and the radiation patches are surrounded by the cavity. The cavity is implemented using laser drilled copper filled stacked micro-vias. The diameter of each micro-via is 80–125 micrometers, and

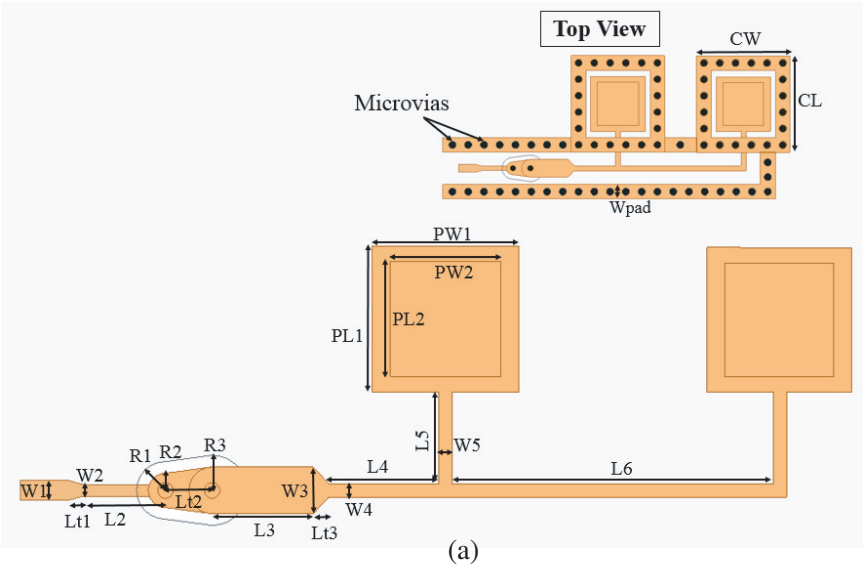

(a)

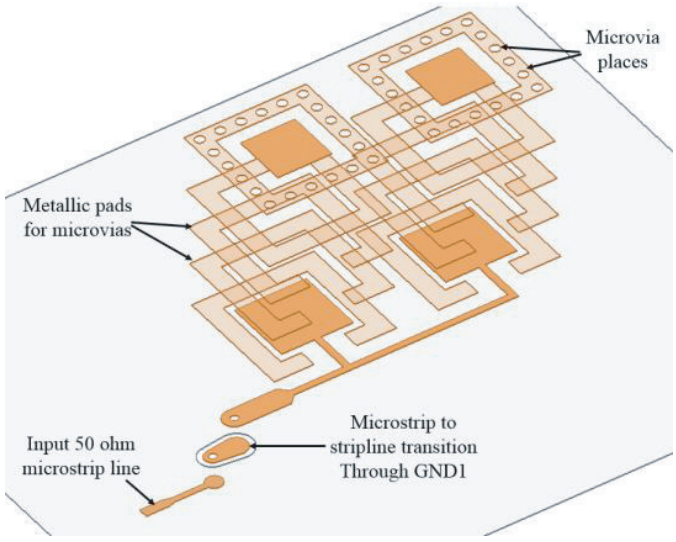

(b)

Figure 4. (a) Sub-array topology: $W1 = 0.13$ mm, $W2 = 0.075$ mm, $L2 = 0.53$ mm, $W3 = 0.3$ mm, $L3 = 0.65$ mm, $W4 = 0.085$ mm, $L4 = 0.7075$ mm, $W5 = 0.085$ mm, $L5 = 0.5875$ mm, $L6 = 2.065$ mm, $Lt1 = Lt3 = 0.1$ mm, $Lt2 = 0.3$ mm, $PW1 = 0.94$ mm, $PL1 = 0.94$ mm, $PW2 = 0.71$ mm, $CW = 1.6$ mm, $CL = 1.65$ mm, $PL2 = 0.74$ mm, $R1 = 0.185$ mm, $R2 = 0.11$ mm, $R3 = 0.2$ mm, $Wpad = 0.25$ mm. (b) Antenna layers.

the pitch between them is 250 micrometer. The top and bottom view of fabricated antenna sub-array are shown in Fig. 5.

Note the 90 degree bent in the feeding network in Fig. 4. The main reason is the fact that the Tx and Rx sub-arrays must be placed in each other's H-plane in order to minimize the coupling between them. The coupling in E-plane is much larger. However, the distance between sub-arrays (in E-plane) must be less than half a wavelength in order to suppress side lobes, as shown in Fig. 11(a). The bending offers a simple solution to be able to do this. Side lobe suppression is very significant in radar applications, since location estimation ambiguity arises with the side lobes.

Although at first the bending may seem to be a straightforward feature without any effect, this modification actually has a serious effect on the antenna. In fact, by bending the feed, electric charges gather in the corner of the bend. In combination with the coupling to the GND2 and the metallic wall surrounding the bend, this acts as a capacitance, which increases the imaginary part of the input impedance. Obviously, this leads to a considerably narrower bandwidth.

The simulated and measured S_{11} of the sub-array are shown in Fig. 6. The simulated S_{11} bandwidth is from 75.25 to 85.99 GHz, which is around 10.7 GHz. The measured S_{11} bandwidth is from 72.43 to 84.6 GHz. Fabrication tolerances on the substrates thicknesses, dimensions, and material characteristics are the typical reasons for this shift. The fabricated antenna dimensions and substrate thicknesses were checked under a microscope. The dimensional tolerances were under 5%. The effect of this level of tolerances on the operating frequency band was explicitly checked through simulations. The shifts are smaller than 1 GHz. The main reason for the 3 GHz shift is the discrepancy between the relative permittivity in the data sheets of the manufacturer, and the actual relative permittivity. This is illustrated by the second simulation (indicated by Sim-changed Er), where all the substrate permittivities of Fig. 2 have been increased by 0.3. The resulting plot very well matches the measurement results. It must be noted that even with this frequency shift, the antenna sub-array still covers the required bandwidth of the intended MIMO (Multi Input Multi Output) radar, with a working frequency band from 77 to 81 GHz.

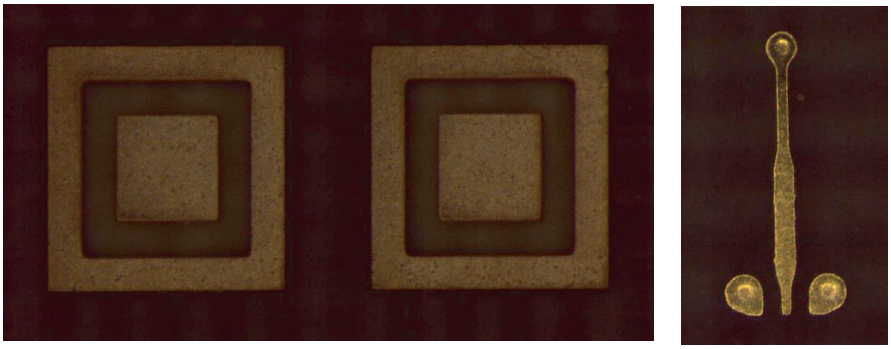

(a) (b)

Figure 5. Fabricated sub-array. (a) Top View. (b) Bottom View.

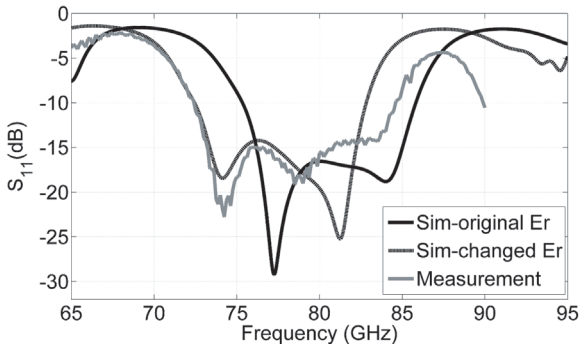

Figure 6. Simulated and measured S_{11} for the sub-array with 2 cavity backed elements.

Radiation pattern measurements were done with the setup described in [19]. The results in E and H-plane for 79 GHz are shown in Fig. 7. The beamwidths in E-plane and H-plane are 136 and 36 degrees, respectively. Since the MIMO radar has been designed for short ranges, this wide beam in E-plane is very helpful. It is used to scan the area in azimuth. There is an excellent agreement between measurements and simulations for the co-polarization, but there is a serious discrepancy for the crosspolarization. This is not different from other such antennas in literature [18]. The possible reasons for this discrepancy are: a slight asymmetry in the fabricated antenna, a small misalignment between the antenna under test and the horn antenna in the measurement set-up, and finally the uncertainty of the measurement itself. The simulated radiation efficiency for this antenna is 83%. The simulated and measured antenna gain are shown in Fig. 8. In this figure, "Sim" is the simulated antenna gain considering the permittivity reported officially by Panasonic, "Sim-Er+0.3" is the simulated antenna gain considering the 0.3 change in the permittivity, and "Meas" is the measured antenna gain. Similar as in the case of S_{11}, the measured antenna gain is very close to the simulated one when adding 0.3 to the permittivity, which further motivates this modification.

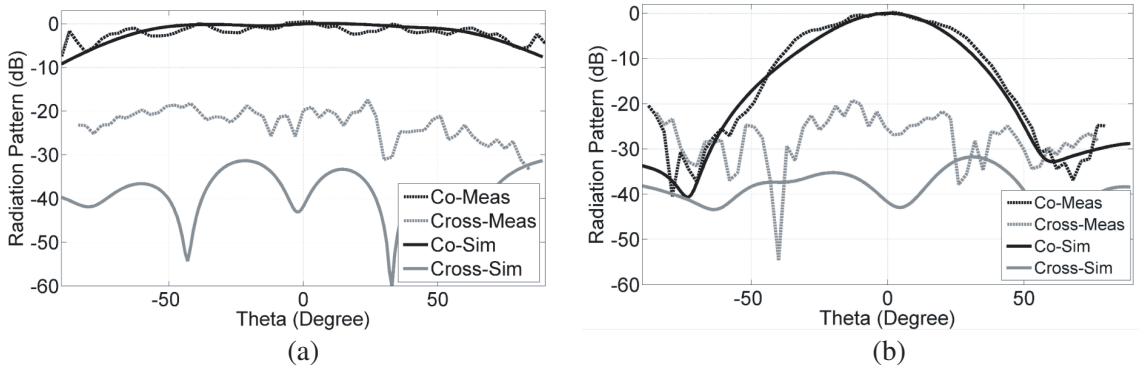

Figure 7. Sub-array radiation pattern in 79 GHz. (a) E plane and (b) H plane.

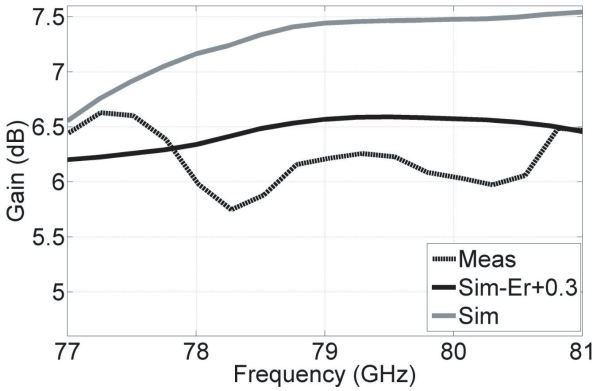

Figure 8. Simulated and measured antenna gain versus frequency.

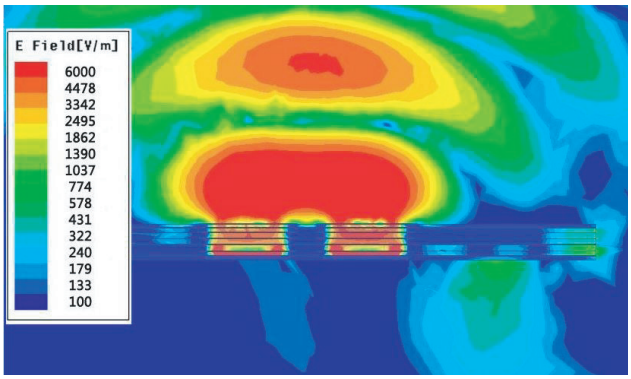

Figure 9. Snapshot of simulated electric field intensity in H-plane in logarithmic scale at 79 GHz.

3.1. Shielding Effectiveness of Package

The simulated electrical field intensity in the H-plane of the sub-array at 79 GHz is illustrated in Fig. 9. This figure clearly shows the near-field radiation emerging from the top patch at the top of the package, and the field intensity reduction at the bottom of the package, which is more than 30 dB lower. As expected, the bottom shielding layer (GND1 in the build-up) has a significant impact on the backside radiation, which allows us to place the chip directly below the radiating elements, thereby decreasing the interconnect length and losses.

3.2. Mutual Coupling in MIMO Radar

The antenna sub-array described above has been used in a PMCW MIMO radar array. The configuration of the MIMO array and the implemented radar module are shown in Figs. 11(a), (b). According to the concept of the virtual array as described in [20], with a spatial convolution of the 4 elements both in the Tx and Rx arrays, a virtual linear array with 16 elements in the receiver part is formed. The key aspect of a MIMO radar system is the use of M orthogonal waveforms each transmitted from different phase centers and N receive phase centers. At each of the receive phase centers, the received signals are matched filtered for each of the transmitted waveforms forming NM channels.

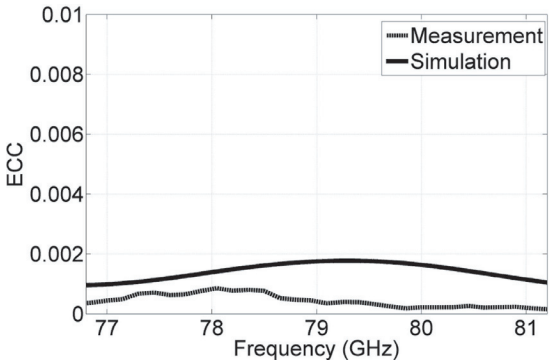

Figure 10. ECC for the MIMO radar system.

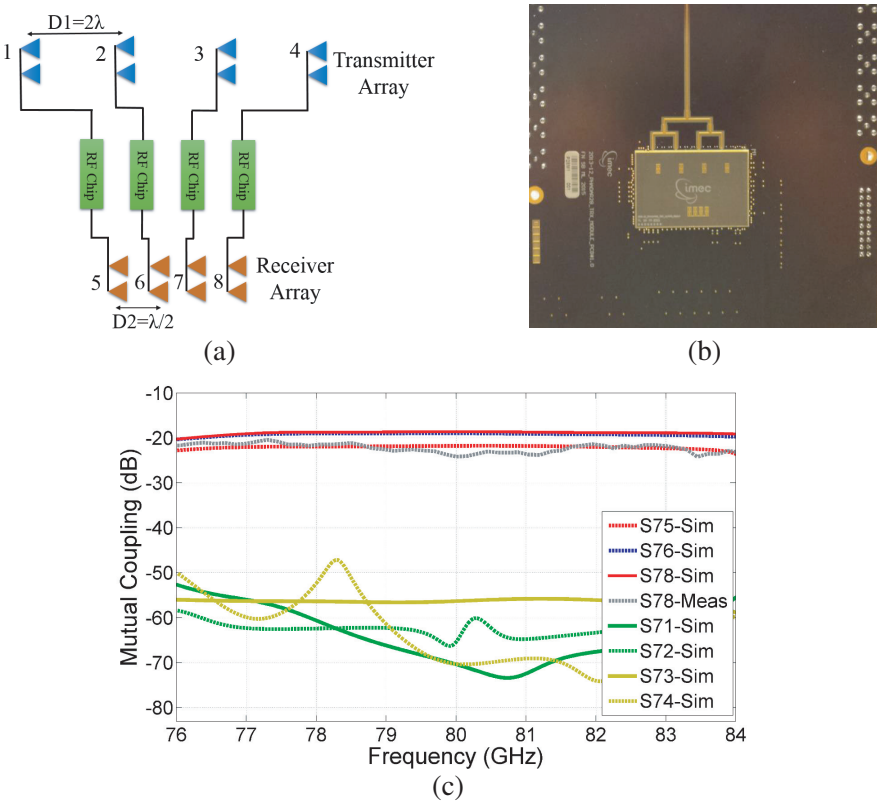

Figure 11. (a) Example of a MIMO radar array where the 2x1 subarray module is used both in Rx and in Tx. The distance between the Rx subarrays is 2.05 mm, which is about half a wavelength in the dielectric. (b) PMCW radar demonstrator. (c) Simulated and measured results for the coupling with subarray 7.

It is evident that since the signal level in the Rx is low, the mutual coupling between the Tx and Rx must be as low as possible. Therefore, it is crucial that the topology is designed in such a way that mutual coupling, especially between Tx and Rx, is very low. In order to demonstrate this, the mutual coupling in the MIMO array of Fig. 11(b) is studied. The simulated mutual couplings between element 7 and other elements in the Rx and Tx array are shown in Fig. 11(c). These values are under -18.8 dB for Rx elements, and are under -47 dB for Tx-Rx elements. Also the level of the values obtained was verified by a measurement between elements 7 and 8. It must be noted that due to the fact that the mutual coupling between the receive and transmit array is extremely low (in the order of -50 dB), it is completely overwhelmed by the inaccuracies which are inevitable in present-day mm-wave measurement setups. For example, state-of-the-art GSG measurement probes may have a considerable parasitic radiation that disturbs the measurement far above a level of -50 dB, see [22]. Hence, the mutual coupling between transmit and receive array could not be measured down to levels of -50 dB.

The Envelope Correlation Coefficient (ECC) is another criterion to assess the isolation of multiple antennas in MIMO systems. Using the definition in [21], this parameter is plotted in Fig. 10. Considering that for MIMO systems, an ECC lower than 0.3 is excellent, it is seen that the ECC for this antenna is extremely low in the 76–82 GHz band.

As mentioned before, the Any-Layer technology provides us with microvias that are quite a bit smaller than through hole vias. Moreover, they can be placed more closely to form the cavity around the patches. This feature provides two main benefits for the MIMO radar. First, this leads to more mitigation of surface waves and mutual coupling. Second, since the microvias are smaller and their pads are very narrow, the antenna elements in Rx can be placed at a distance very close to half a wavelength, which avoids side grating lobes.

4. CONCLUSION

In this paper, a new cavity backed stacked patch antenna topology for 79 GHz MIMO radar applications is introduced. The antenna is fabricated with a low cost high resolution advanced Any-Layer PCB technology. Reflection coefficient and radiation pattern measurement and simulation results show a good agreement. The antenna topology has a very wide beamwidth in both E plane (more than 135 degrees) and H plane. These wide beam widths are necessary for short range radars. The impedance bandwidth is more than 13.5%, which completely fulfills the requirements of radar applications in the 79 GHz band. In contrast to topologies already described in literature, the wide bandwidth is achieved with small elements (smaller than half a wavelength) and without embedding air cavities into the build-up, which enhances both the complexity and cost. In addition, due to a novel and wideband feed transition from microstrip to stripline, the radiation to the chip side has been reduced by more than 30 dB. Furthermore, thanks to the small and high resolution microvias provided by the Any-Layer technology, a low mutual coupling below -18.8 dB is reached over the whole radar bandwidth, without using extra structures like EBG or DGS.

REFERENCES

1. Cui, B., C. Wang, and X.-W. Sun, "Microstrip Array Double-Antenna (MADA) technology applied in millimeter wave compact radar front-end," *Progress In Electromagnetics Research*, Vol. 66, 125–136, 2006.
2. Camblor-Diaz, R., S. Ver-Hoeye, C. Vazquez-Antuna, G. R. Hotopan, M. Fernandez-Garcia, and F. Las Heras Andres, "Sub-millimeter wave frequency scanning 8×1 antenna array," *Progress In Electromagnetics Research*, Vol. 132, 215–232, 2012.
3. Hasch, J., E. Topak, R. Schnabel, T. Zwick, R. Weigel, and C. Waldschmidt, "Millimeter-wave technology for automotive radar sensors in the 77 GHz frequency band," *IEEE Trans. Microw. Theory Techn.*, Vol. 60, No. 3, Part 2, 845–860, 2012.
4. Guermandi, D., Q. Shi, A. Medra, T. Murata, W. Van Thillo, A. Bourdoux, P. Wambacq, and V. Giannini, "A 79 GHz binary phase-modulated continuous-wave radar transceiver with TX-to-RX

spillover cancellation in 28 nm CMOS," *2015 IEEE International Solid-State Circuits Conference (ISSCC)*, 1–3, 2015.

5. Wong, K. W., L. Chiu, and Q. Xue, "A 2-D van atta array using star-shaped antenna elements," *IEEE Trans. Antennas Propag.*, Vol. 55, No. 4, 1204–1206, 2007.
6. Yousefzadeh, N., C. Ghobadi, and M. Kamyab, "Consideration of mutual coupling in a microstrip patch array using fractal elements," *Progress In Electromagnetics Research*, Vol. 66, 41–49, 2006.
7. Farahbakhsh, A., M. Mosalanejad, Gh. Moradi, and Sh. Mohanna, "Using polygonal defect in ground structure to reduce mutual coupling in microstrip array antenna," *Journal of Electromagnetic Waves and Applications*, Vol. 28, No. 2, 194–201, 2014.
8. Ghosh, C. K., B. Mandal, and S. K. Parui, "Mutual coupling reduction of a dual frequency microstrip antenna array by using U-shaped DGS and inverted U-shaped microstrip resonator," *Progress In Electromagnetics Research C*, Vol. 48, 61–68, 2014.
9. Islam, M. T. and M. S. Alam, "Compact EBG structure for alleviating mutual coupling between patch antenna array elements," *Progress In Electromagnetics Research*, Vol. 137, 425–438, 2013.
10. Yang, X. M., X. G. Liu, X. Y. Zhou, and T. J. Cui, "Reduction of mutual coupling between closely packed patch antennas using waveguided metamaterials," *IEEE Antennas Wireless Propag. Lett.*, Vol. 11, 389–391, 2012.
11. Qamar, Z. and H. C. Park, "Compact waveguided metamaterials for suppression of mutual coupling in microstrip array," *Progress In Electromagnetics Research*, Vol. 149, 183–192, 2014.
12. Li, Y. and K.-M. Luk, "60-GHz substrate integrated waveguide fed cavity-backed aperture-coupled microstrip patch antenna arrays," *IEEE Trans. Antennas Propag.*, Vol. 63, No. 3, 1075–1085, 2015.
13. Ou Yang, J., S. Bo, J. Zhang, and F. Yang, "A low-profile unidirectional cavity-backed log-periodic slot antenna," *Progress In Electromagnetics Research*, Vol. 119, 423–433, 2011.
14. Kam, D., D. Liu, A. Natarajan, S. Reynolds, H. Chen, and B. A. Floyd, "LTCC packages with embedded phased-array antennas for 60 GHz communications," *IEEE Antennas Wireless Propag. Lett.*, Vol. 21, No. 3, 142–144, 2011.
15. Pazin, L. and Y. Leviatan, "A compact 60-GHz tapered slot antenna printed on LCP substrate for WPAN applications," *IEEE Antennas Wireless Propag. Lett.*, Vol. 9, 272–275, 2010.
16. Brebels, S., Ch. Soens, W. De Raedt, and G. A. E. Vandenbosch, "Compact LTCC antenna package for 60 GHz wireless transmission of uncompressed video," *IEEE MTT-S International Microwave Symposium Digest*, 1–4, 2011.
17. Liu, D., J. A. G. Akkermans, H. Chen, and B. Floyd, "Packages with integrated 60-GHz aperture-coupled patch antennas," *IEEE Trans. Antennas Propag.*, Vol. 59, No. 10, 3607–3616, 2011.
18. Enayati, A., G. A. E. Vandenbosch, and W. De Raedt, "Millimeter-wave horn-type antenna-in-package solution fabricated in a teflon-based multi-layer PCB technology," *IEEE Trans. Antennas Propag.*, Vol. 61, No. 4, 1581–1590, 2013.
19. Mosalanejad, M., S. Brebels, I. Ocket, V. Volski, C. Soens, and G. A. E. Vandenbosch, "A complete measurement system for integrated antennas at millimeter wavelengths," *9th European Conference on Antennas and Propagation (EuCAP)*, 1–5, 2015.
20. Haimovich, A., R. Blum, and L. Cimini, "MIMO radar with widely separated antennas," *IEEE Signal Process. Mag.*, Vol. 25, No. 1, 116–129, 2008.
21. Blanch, S., J. Romeu, and I. Corbella, "Exact representation of antenna system diversity performance from input parameter description," *Electronics Letters*, Vol. 39, No. 9, 705–707, 2003.
22. Mohammadpour-Aghdam, K., S. Brebels, A. Enayati, R. Faraji-Dana, G. Vandenbosch, and W. DeRaedt, "RF probe influence study in millimeterwave antenna pattern measurements," *International Journal of RF and Microwave Computer-aided Engineering*, Vol. 21, No. 4, 413–420, 2011.
23. Aspocomp PCB technology, Keilaranta, Finland, Website: "https://www.aspocomp.com".